Investigating Unsupervised Machine-Learning Classification of British Columbia Copper-Porphyry Ore and Indicator Minerals Using Micro-X-Ray–Fluorescence Core Scanners

B. Eaton[1], **Department of Earth, Ocean and Atmospheric Sciences, The University of British Columbia, Vancouver, British Columbia, beaton@eoas.ubc.ca**

A. Steiner, Department of Earth, Ocean and Atmospheric Sciences, The University of British Columbia, Vancouver, British Columbia

S. Barker, Department of Earth, Ocean and Atmospheric Sciences, The University of British Columbia, Vancouver, British Columbia

L. Heagy, Department of Earth, Ocean and Atmospheric Sciences, The University of British Columbia, Vancouver, British Columbia

Eaton, B., Steiner, A., Barker, S. and Heagy, L. (2023): Investigating unsupervised machine-learning classification of British Columbia copper-porphyry ore and indicator minerals using micro-X-ray–fluorescence core scanners; *in* Geoscience BC Summary of Activities 2022: Minerals, Geoscience BC, Report 2023-01, p. 37–44.

Introduction

Copper-porphyry deposits are large-tonnage, low-grade, intrusive mineral deposits that range from less than 10 Mt to 10 Gt grading 0.5 to 1.5% Cu (Sillitoe, 2010). Copper-porphyry systems host over three-quarters of the global copper resources and are thus a vital source for meeting the world's current and future copper demand (Sillitoe, 2010). As the world transitions to a decarbonized economy, copper is increasingly required to support global electrification upgrades to industrial systems as well as transportation and low-carbon energy infrastructure. The increasing global population and infrastructure-electrification upgrades will cause the global demand for copper to rise by a predicted 275% to 350% by 2050 (Elshkaki et al., 2016; Ciacci et al., 2020). New mineral-deposit discoveries are critical to meeting this demand; however, the remaining undiscovered deposits are in regions that are mostly or entirely hidden under hundreds of metres of postmineral cover material (Gonzalez-Alvarez et al., 2020). Exploring through postmineral cover adds significant complications and challenges to the discovery of new mineral deposits (Eppinger et al., 2013). Effective, timely and economically feasible exploration technologies must be developed to meet the rise in copper demand and address the challenges associated with exploring under increasing depths of postmineral cover (Gonzalez-Alvarez et al., 2020).

This research will contribute to the development of cost-effective, efficient and quantitative exploration techniques for porphyry-copper exploration under sedimentary cover material in British Columbia (BC) and will be applicable to any exploration program utilizing detrital indicator-mineral (DIM) methods. The research objectives of the project are to improve, quantify and expedite the identification of copper ore and gangue minerals, focusing primarily on Cu-porphyry DIMs, using methods that will be developed on samples from Cu-porphyry exploration programs and producing Cu-porphyry mines in BC. The research objectives will be achieved by developing a quantitative approach to indicator-mineral identification that overcomes the limitations of conventional DIM methods that include the handpicking of mineral grains and prohibitive costs associated with scanning electron microscope (SEM) analysis. The aim of the research is to develop Cu-porphyry DIM-identification methods using benchtop micro-X-ray–fluorescence (μXRF) core scanners. The μXRF DIM-identification methods will be evaluated against SEM analysis of samples from producing BC Cu-porphyry mines and Cu-porphyry exploration programs.

Background Information

Indicator Minerals

Indicator minerals are minerals that contain textural or chemical information indicating the presence of specific mineralization in the bedrock from which the minerals originally came (McClenaghan et al., 2000). In Cu-porphyry exploration, indicator minerals have been widely used as geochemical and detrital vectoring tools (Eppinger et al., 2013; Cooke et al., 2020). Detrital indicator minerals are derived from sediments such as glacial till, stream and lake sediments, or soil samples. Detrital indicator minerals have been used to explore for various mineral resources in-

[1] *The lead author is a 2022 Geoscience BC Scholarship recipient.*

This publication is also available, free of charge, as colour digital files in Adobe Acrobat® PDF format from the Geoscience BC website: http://geosciencebc.com/updates/summary-of-activities/.

cluding diamonds, gold, precious gems, base-metal sulphides and Cu–Ni–platinum-group element sulphides (McClenaghan, 2005; Gent et al., 2011). The use of DIMs has led to the discovery of numerous Canadian deposits and DIM methods can also be used to explore for Cu-porphyries in BC (Plouffe et al., 2016).

Detrital Indicator-Mineral Methods

Methods that rely on DIMs generally involve sampling, phase segregation and handpicking under an optical microscope by a human expert and/or SEM analysis (McClenaghan and Layton-Matthews, 2017). Optical grain counting and handpicking DIMs is labour intensive, inherently human biased and subjective, and results in both costly and slow analysis compared to automated mineralogical methods (Gent et al., 2011; Sylvester, 2012). Automated mineralogy using SEM analysis has been widely applied to DIMs; the method offers improvements in repeatability, quantification and automation (Lougheed et al., 2020). The challenges to applying widespread automated SEM analysis to a DIM exploration program are the high costs associated with the method and the relatively long amount of time required for sample preparation, analysis and data interpretation.

Benchtop µXRF Core Scanners

Analysis of DIMs by high-resolution µXRF core scanners offers a promising alternative to SEM-based methods, or may be complementary to these methods, when applied to DIMs. High-resolution (in the order of tens of microns) µXRF core scanners have been widely used by the paleoclimate scientific community to investigate paleosediment cores for the past two decades (Jansen et al., 1998). The µXRF analytical approaches used in paleoclimate research are increasingly being applied to the geosciences and mineral and petroleum industries (Croudace et al., 2019). Geological applications include sedimentary-core trace-metal analysis (Hennekam et al., 2019), characterization of volcanic debris (Peti et al., 2019) and mineral mapping in Carlin-type gold systems (Barker et al., 2021). The petroleum and mining industries have used benchtop µXRF analysis for tailings characterization (Fawcett and Jamieson, 2011; Galloway et al., 2018), tying of geochemical signatures to mechanical properties of rocks (Hussain et al., 2018) and geochemical characterization of stratigraphy in unconventional reservoirs (Hussain et al., 2022). Use of µXRF core scanners presents an opportunity to rapidly characterize DIMs to aid in the search for Cu-porphyry deposits.

Automated Mineral Identification

Artificial intelligence and machine-learning (ML) applications have undergone widespread innovation in mining and the geological sciences in the past ten years (Jooshaki et al., 2021). Machine learning is an area of study with a set of methods that extracts meaningful patterns and associations from known information that can be generalized and applied to new data to make predictions under uncertainty (Jordan and Mitchell, 2015). The ML methods investigated in this study can broadly be grouped into two categories: supervised and unsupervised methods. Supervised ML methods are a broad family of algorithms that are first trained on labelled data and then applied to predict labels on test or new data, whereas unsupervised ML methods are applied to unlabelled data. Structural and relational properties within the data are extracted by unsupervised methods and these relationships are used to cluster or reduce the dimensionality of the dataset (Jordan and Mitchell, 2015).

Automated mineral identification has been widely implemented in mining and the geosciences since the early 2000s using automated scanning electron microscopy (Gottlieb et al., 2000). Automated mineral-identification methods can also be grouped into two theoretical approaches: supervised classification methods using mineral standard-spectral libraries and unsupervised clustering methods (Schulz et al., 2020; Jooshaki et al., 2021). Automated SEM analysis predominantly identifies minerals by comparing the energy dispersive spectroscopy (EDS) spectra of a phase to known EDS spectra in a mineral standard-spectral library to determine the best match. Alternatively, phases can be identified without a mineral standard-spectral library by resorting instead to unsupervised clustering of similar EDS spectra into distinct separate groupings representing phases present in the sample. Unsupervised clustering allows for phases to be identified without building an extensive database; however, the method still requires user input to relate clusters of similar spectra to the mineral(s) that generated them. Furthermore, there is widespread potential to apply modern supervised and unsupervised methods to EDS spectra and other electron-microbeam analyses used to identify minerals, including µXRF (Jooshaki et al., 2021). For example, supervised neural networks have been applied to generate mineral maps by classifying integrated µXRF and micro-X-ray–diffraction (µXRD) data of fine-grained shale units to model mineral reactivity (Kim et al., 2022).

Methodology

Geochemical µXRF Analysis

An M4 Tornado Plus benchtop µXRF core scanner, manufactured by Bruker and equipped with a rhodium tube and two 260 mm^2 silicon drift EDS detectors with ultra-thin windows, was used for the analysis. Standard analytical parameters of 19 µm X-ray beam width, 100 µm pixel resolution, 10 ms/pixel dwell time, double detector channels, 50 kV acceleration voltage and chamber pressure of 1 mbar

were used. The M4 Tornado Plus has a mapping area of 190 by 160 mm.

Benchtop µXRF core scanners nondestructively analyze whole-rock samples producing two-dimensional arrays of XRF spectra (Flude et al., 2017). A two-dimensional array of XRF spectra per pixel was produced representing the geochemical variation across the sample. Chemical maps, also commonly referred to as 'elemental maps', were produced by matching elemental peaks to the XRF spectral peaks identified in the scanned XRF spectra from the bulk composition of the sample. Areas of interest were selected for later quantification using the M4 Tornado Plus software package.

Elemental quantification was completed in the Bruker ESPRIT 2.4 software. The ESPRIT software is more efficient in quantifying elemental concentrations to acquire large chemical maps than the M4 software due to its multicore processing capabilities. Normalized, quantitative elemental abundances were derived for each pixel from the XRF spectra using the 'oxides' quantification method from the Bruker Quantitative Mapping (QMap) tool, which relies on fundamental-parameters standardless quantification to determine elemental concentrations from the XRF spectra (Kanngieβer, 2003). Fundamental-parameters standardless-XRF quantification has been determined to be the best quantification method for heterogeneous rock samples due to the high geochemical variation found within geological material (Flude et al., 2017; Barker et al., 2021). Future work will validate the use of this method applied to Cu-porphyry DIMs. Both quantified and normalized elemental-concentration data were collected.

Exploratory Data Analysis

Exploratory data analysis of the quantified chemical maps was completed in Python, a high-level programming language. A dimension-reduction algorithm was used to transform the quantified compositional data from multidimensional elemental space to two-dimensional space. An unsupervised ML clustering method was applied to the transformed two-dimensional data to identify distinct clusters. The mineral names or mineral groups represented by similar compositional clusters were determined by the bulk chemistry of the cluster. Quantified elemental and mineral maps were produced using a data-visualization package.

Samples

A 5 by 16 cm piece of granitic Cu-porphyry core was scanned with a Bruker M4 Tornado Plus core scanner at the Electron Microbeam and X-Ray Diffraction Facility (Vancouver, BC), associated with the Mineral Deposit Research Unit of The University of British Colombia (Figure 1). The sample was mineralized with chalcopyrite and pyrite recognized in hand sample. Gangue minerals present in the sample were quartz, feldspar, amphibole and mica. A mosaicked RGB image of the sample was captured at 100x magnification (Figure 1); the area of the sample shown in the inset on Figure 1 was selected for chemical quantification and normalization.

Preliminary Results

Chemical Maps

Using a visualization package in Python, chemical maps were produced from exported quantified and normalized elemental concentrations determined using the Bruker ESPRIT QMap tool. Preliminary quantified chemical maps of Si, Al, K, Ca, Mg and P are shown in Figure 2, while S, Cu and Fe are presented in Figure 3. The µXRF chemical maps of geological material represent the relative geochemical variations within a sample, which are controlled by the distribution and composition of minerals in the sample (Barker et al., 2021). For example, the Si and Al chemical maps clearly show quartz veins surrounded by an

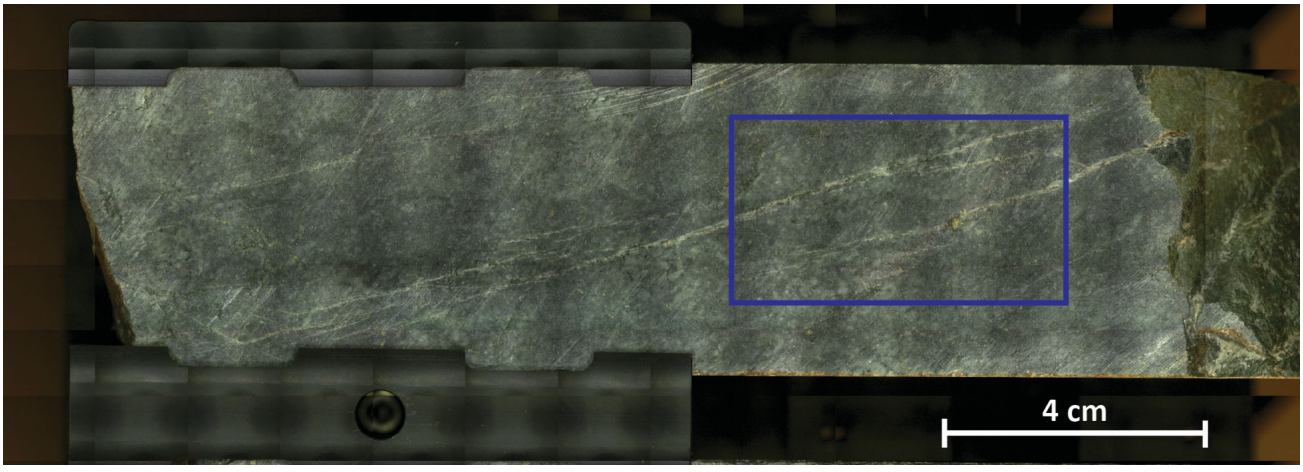

Figure 1. Mosaic of the Cu-porphyry core captured by the camera in the chamber of the Bruker M4 Tornado Plus core scanner (inset shows area that was selected for quantification).

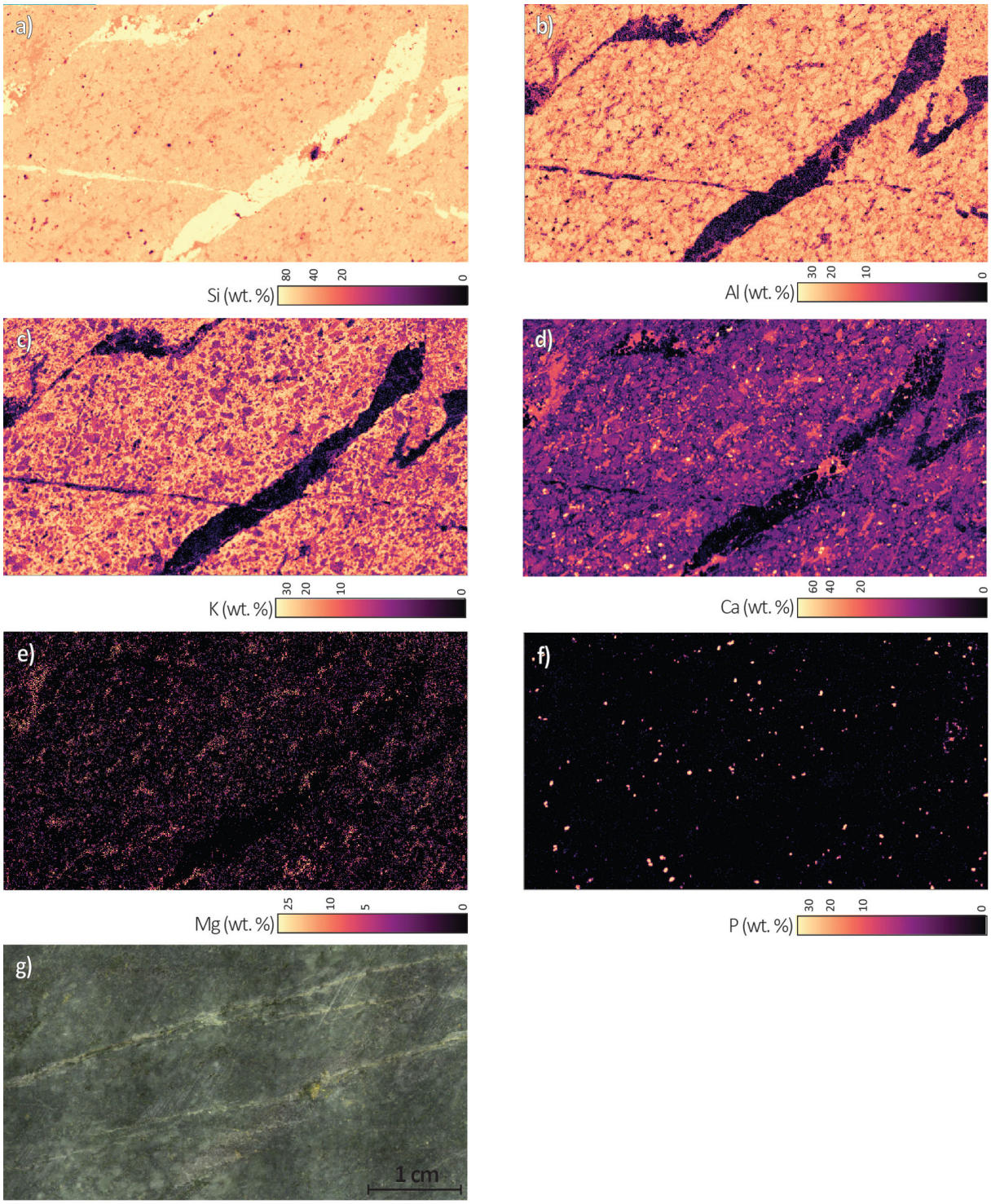

Figure 2. Micro-X-ray–fluorescence images showing quantified concentrations of Si **(a),** Al **(b),** K **(c),** Ca **(d),** Mg **(e)** and P **(f)** in a mineralized Cu-porphyry core sample **(g)** shown in an image captured at 100x magnification by the camera of a Bruker M4 Tornado Plus core scanner. The µXRF chemical maps represent the geochemical variations within a sample, which are controlled by the distribution and composition of minerals in the sample. The Si and Al chemical maps clearly show quartz veins surrounded by an aluminosilicate matrix (Figure 2a, b). The Ca chemical map illustrates several groupings of Ca-bearing minerals in the aluminosilicate matrix (Figure 2d). The highest Ca values overlap with the highest P values (Figure 2f) indicating the presence of apatite $\{Ca_5(PO_4)_3(F,Cl,OH)\}$; moderate Ca, Mg and Fe values and elongate crystal shapes indicate hornblende $\{Ca_2(Mg,Fe,Al)_5(Al,Si)_8O_{22}(OH)_2\}$ is present; moderate to low Ca values with Al indicate the presence of plagioclase feldspar $\{(Na,Ca)Al_2Si_2O_8\}$; and very low to no Ca indicates that quartz is present. Additionally, the K elemental map shows the effects of potassic-hydrothermal alteration, associated with the ore zone, where high K values indicate potassic alteration in the aluminosilicate gangue (Figure 2c). Chemical maps were produced using a visualization package in the programming language Python from exported quantified and normalized elemental concentrations determined using the Bruker ESPRIT QMap tool.

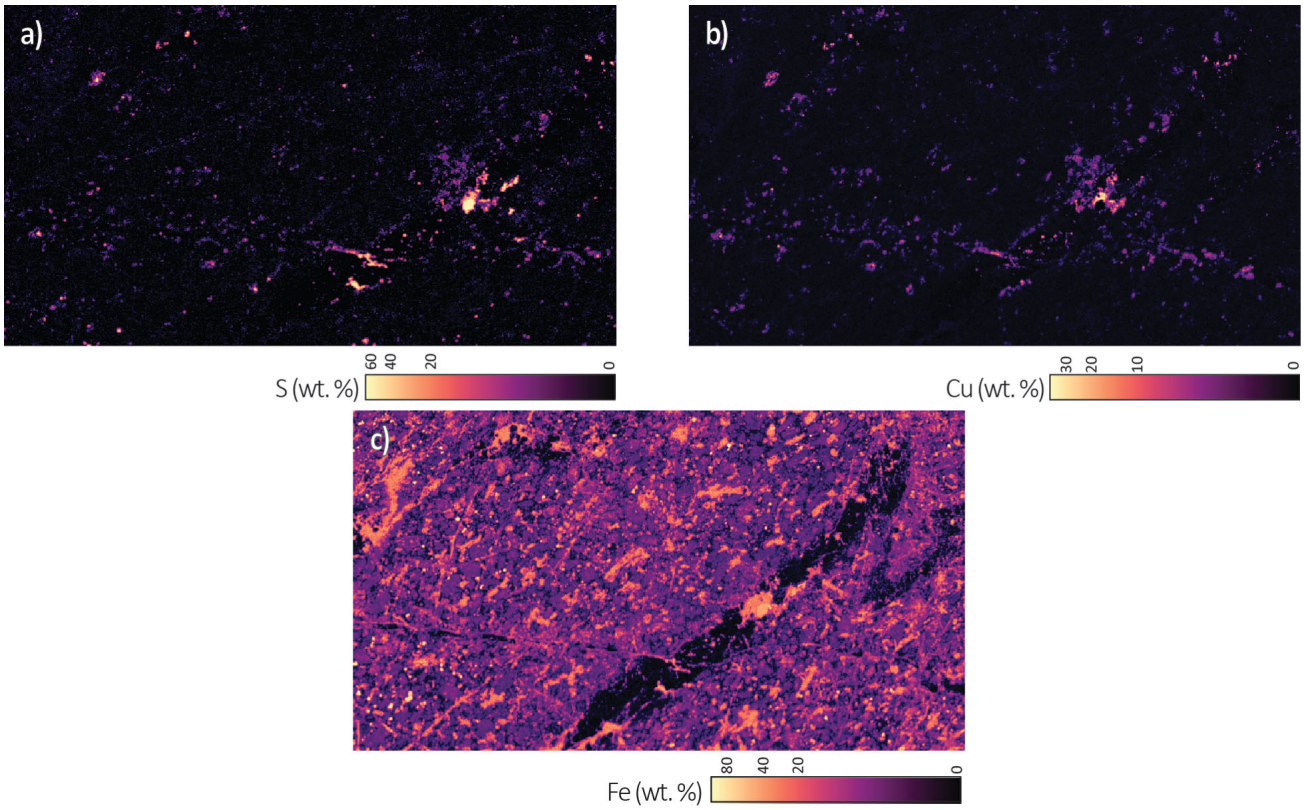

Figure 3. Micro-X-ray–fluorescence images showing quantified concentrations of S **(a)**, Cu **(b)** and Fe **(c)** in a mineralized Cu-porphyry core sample. Copper-ore minerals and sulphide gangue can be readily identified by S, Fe and Cu values on the chemical maps. The high Cu values indicate the presence of chalcopyrite and high Fe and S values, that of pyrite.

aluminosilicate matrix (Figure 2a, b). Similarly, copper-ore minerals and sulphide gangue can be readily identified by S, Cu and Fe values on the chemical maps (Figure 3). The high Cu values indicate the presence of chalcopyrite, and high Fe and S values indicate that of pyrite. In addition to identifying mineralization and vein composition, the chemical maps can be used to visualize the elemental variance across a sample to determine mineralogy and hydrothermal alteration in the quartz-aluminosilicate matrix. For example, the quantified Ca chemical map illustrates several groupings of Ca-bearing minerals (Figure 2d). The highest Ca values overlap with the highest P values (Figure 2f) indicating the presence of apatite $\{Ca_5(PO_4)_3(F,Cl,OH)\}$; moderate Ca, Mg and Fe values and elongate crystal shapes indicate that hornblende $\{Ca_2(Mg,Fe,Al)_5(Al,Si)_8O_{22}(OH)_2\}$ is present; moderate to low Ca values with Al indicate the presence of plagioclase feldspar $\{(Na,Ca)Al_2Si_2O_8\}$; and very low to no Ca indicates that quartz is present. In addition to mineralogy, the chemical effects of hydrothermal alteration can be seen on the chemical maps (Figure 2c). High K values in the aluminosilicate matrix illustrate widespread potassic alteration, where K has replaced Ca and Na in the gangue minerals (Figure 2c).

Mineral Maps

The unsupervised clustering algorithm identified six clusters that generally correspond to chalcopyrite, pyrite, hornblende, apatite, quartz and aluminosilicate-quartz matrix (Figure 4). Apatite, chalcopyrite and pyrite were compositionally distinct and easily separated using the clustering algorithm. The clustering algorithm was not as effective when used to separate compositionally similar aluminosilicate mineral groups, such as feldspar and clay.

Discussion

µXRF Chemical Mapping

The benchtop µXRF core scanner and ESPRIT QMap tool used to quantify elemental maps displayed in Python were highly effective in producing informative chemical maps for ore, gangue and indicator minerals. The maps clearly illustrated vein mineralogy and highlighted copper-mineralization distribution across the sample. Quartz veins can be identified by high Si values, whereas copper-ore minerals and pyrite gangue can be readily identified by S, Fe and Cu, and the aluminosilicate matrix can be differentiated by Ca concentration (Figures 2, 3). High P values highlighted apatite grains, a key porphyry-indicator mineral (Bouzari et al., 2016). Hydrothermal alteration is another example of

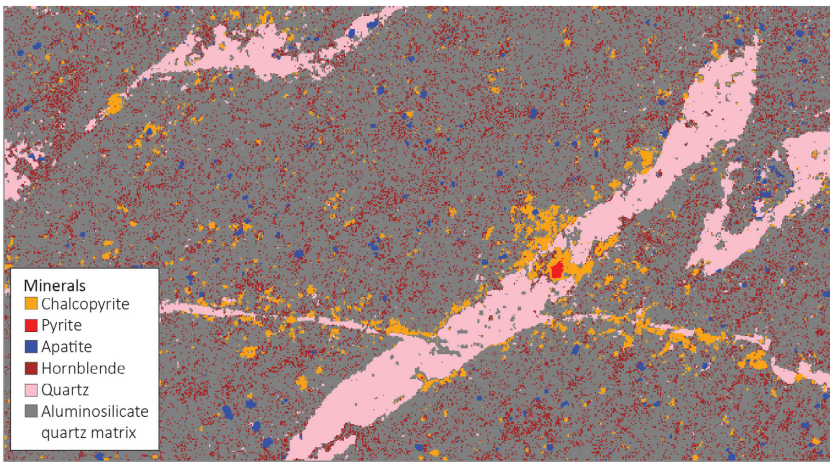

Figure 4. Mineral map of a mineralized Cu-porphyry core sample derived from quantified micro-X-ray–fluorescence chemical maps using unsupervised dimensionality-reduction and clustering methods. The unsupervised clustering algorithm identified six distinct clusters that generally correspond to chalcopyrite, pyrite, apatite, hornblende, quartz and aluminosilicate-quartz matrix. Apatite, chalcopyrite and pyrite were compositionally distinct and easily separated using the clustering algorithm; however, fine pyrite grains may have been underestimated. The clustering algorithm was less effective in separating compositionally similar aluminosilicate mineral groups, such as feldspar and clay. The copper mineralization illustrated on the mineral map is predominantly associated with, or proximal to, quartz veining and the sulphides present are chalcopyrite and pyrite. Apatite, a key Cu-porphyry–indicator mineral, can be readily identified on the mineral map.

µXRF chemical mapping revealing subtle geochemical textures. The µXRF chemical maps of the porphyry core show widespread elevated values of K (Figure 2c) that are interpreted to indicate pervasive potassic alteration with K replacement in aluminosilicates.

µXRF Mineral Identification

In this study, copper mineralization, sulphides, amphibole and apatite were successfully clustered into distinct groupings by the unsupervised clustering method and a user-assigned mineral name from the bulk chemistry of the cluster was given to the cluster. As this work is preliminary, the mineral phases identified require future external validation by scanning electron microscopy and/or X-ray diffraction (XRD). The clustering method applied functions most effectively when determining compositionally distinct minerals such as chalcopyrite, pyrite, apatite and quartz. These groupings were easily separated using the clustering algorithm, although this method failed when used to separate the minerals in the aluminosilicate matrix, such as feldspar, clay and amphibole. Additional work refining and developing the clustering method is required to distinguish between compositionally similar aluminosilicate groups, such as has been achieved using the linear-programming approach adopted by Barker et al (2021). The difficulty in identifying compositionally similar minerals is not unique to µXRF chemical mapping. Compositionally similar minerals, such as aluminosilicates and oxides, pose a challenge to electron-microbeam–derived spectral methods of mineral identification as these minerals are difficult to distinguish one from the other due to the fact their similar spectra reflect similar elemental compositions.

µXRF Technical Challenges

Several technical challenges were identified in this study. Mixed XRF spectra were a potential drawback of the method and posed an additional challenge when it came to identifying minerals using µXRF chemical mapping. The large excitation volume of the electron beam can produce deep multiphase fluorescence and result in horizontal and vertical spectral mixing in nonmonolayered samples (Flude et al., 2017). For example, neighbouring minerals adjacent to, and lying below, the uppermost mineral in a sample may interact with the electron beam and result in mixed spectra. Spectral mixing can result in an apparent range of compositions for a mineral due to the effect of neighbouring minerals diluting the signal from the mineral of interest. Two-phase mixing may be readily quantified, however, three- to four-phase mixing greatly complicates deconvolution of the µXRF spectra when determining quantified mineralogy (Barker et al., 2021). Mixed pixels consisting of spectra from two or more minerals complicated the clustering algorithm's effectiveness in separating mineral groups by composition. This was due to mineral chemical compositions appearing to range from the end-member chemistry of a mineral, derived from unmixed spectra, to a blend of the chemical compositions of two or more minerals, derived from mixed spectra. The apparent range of mineral compositions that blended into one another reduced the effectiveness of the clustering algo-

rithm to distinguish between separate, distinct mineral groups.

μXRF Geoscience and Exploration Applications

Micro-X-ray–fluorescence techniques provide a nondestructive method that can be used for the analysis of major and trace elements; furthermore, these techniques present a wide range of opportunities for applications in the geosciences and mineral exploration (Croudace et al., 2019). Benchtop μXRF core scanners allow for relatively rapid quantitative chemical analysis over a large mapping area, in comparison with other automated mineralogy methods, and can provide key geochemical information at the scale of tens of microns (Flude et al., 2017). For example, μXRF chemical maps can be used to identify mineralogical and compositional variation in veins, provide information on trace precious metals in ores and deleterious elemental distributions in tailings (Fawcett and Jamieson, 2011; Ryan et al., 2018; Barker et al., 2021). Additionally, mineral identification can be derived from μXRF spectra and has widespread potential to aid in DIM exploration programs. Mineral mapping using μXRF results in faster and cheaper analysis requiring less sample-preparation time when compared to automated SEM analyses. However, a consequence of this approach is that the data interpretation becomes more complicated due to the effects of mixed spectra and the difficulty distinguishing between compositionally similar minerals. Machine-learning methods offer opportunities to address the challenges associated with μXRF-data interpretation (Barker et al., 2021; Kim et al., 2022). The preliminary results show that the unsupervised ML methods applied in this study identified key copper ore, gangue and indicator minerals, but were less effective when it came to separating compositionally similar minerals or mixed spectra, thus requiring user input to link clusters to mineral groups. Supervised ML methods can potentially lead to the successful classification of complicated μXRF data as the algorithms can be trained to identify mixed signals and integrate additional datasets, such as those obtained from XRD, optical images or microscopy (Barker et al., 2021; Kim et al., 2022).

Conclusion

The aims of this research are to develop μXRF mineral-identification methods designed to improve, quantify and expedite the identification of Cu-porphyry–related ore, gangue and indicator minerals. The project will contribute to the development of industry-applicable, cost-effective quantitative mineral-identification methods. The preliminary study investigated mineral-identification methods on a piece of mineralized Cu-porphyry core using μXRF chemical mapping and unsupervised ML methods. The unsupervised mineral-identification methods identified copper mineralization, sulphides and porphyry-indicator minerals, including chalcopyrite and apatite. Compositionally similar minerals, such as aluminosilicates, were not readily identified using the clustering method. These preliminary results show the unsupervised ML methods were successful in identifying copper ore and DIMs. Further work is required to validate the μXRF fundamental-parameters standardless quantification of Cu-porphyry minerals and to externally validate the minerals identified by SEM and/or XRD analysis using the clustering algorithm. Future work will apply μXRF chemical mapping and unsupervised ML classification methods to DIMs.

Acknowledgments

The authors thank Geoscience BC, the Society of Economic Geologists and the Mineral Deposits Research Unit of The University of British Columbia for their financial support of this project. The authors would also like to thank J. Saylor for his input and review of the manuscript.

References

Barker, R.D., Barker, S.L.L., Wilson, S.A. and Stock, E.D. (2021): Quantitative mineral mapping of drill core surfaces I: a method for μXRF mineral calculation and mapping of hydrothermally altered, fine-grained sedimentary rocks from a Carlin-type gold deposit; Economic Geology, v. 116, no. 4, p. 803–819, URL <https://doi.org/10.5382/ECONGEO.4803>.

Bouzari, F., Hart, C.J.R., Bissig, T. and Barker, S. (2016): Hydrothermal alteration revealed by apatite luminescence and chemistry; a potential indicator mineral for exploring covered porphyry copper deposits; Economic Geology, v. 111, no. 6, p. 1397–1410, URL <https://doi.org/10.2113/econgeo.111.6.1397>.

Ciacci, L., Fishman, T., Elshkaki, A., Graedel, T.E., Vassura, I. and Passarini, F. (2020): Exploring future copper demand, recycling and associated greenhouse gas emissions in the EU-28; Global Environmental Change, v. 63, art. 102093, URL <https://doi.org/10.1016/J.GLOENVCHA.2020.102093>.

Cooke, D.R., Wilkinson, J.J., Baker, M., Agnew, P., Phillips, J., Chang, Z., Chen, H., Wilkinson, C.C., Inglis, S., Hollings, P., Zhang, L., Gemmell, J.B., White, N.C., Danyushevsky, L. and Martin, H. (2020): Using mineral chemistry to aid exploration: a case study from the Resolution porphyry Cu-Mo deposit, Arizona; Economic Geology, v. 115, no. 4, p. 813–840, URL <https://doi.org/10.5382/econgeo.4735>.

Croudace, I.W., Löwemark, L., Tjallingii, R. and Zolitschka, B. (2019): Current perspectives on the capabilities of high resolution XRF core scanners; Quaternary International, v. 514, p. 5–15, URL <https://doi.org/10.1016/j.quaint.2019.04.002>.

Elshkaki, A., Graedel, T.E., Ciacci, L. and Reck, B.K. (2016): Copper demand, supply, and associated energy use to 2050; Global Environmental Change, v. 39, p. 305–315, URL <https://doi.org/10.1016/J.GLOENVCHA.2016.06.006>.

Eppinger, R.G., Fey, D.L., Giles, S.A., Grunsky, E.C., Kelley, K.D., Minsley, B.J., Munk, L. and Smith, S.M. (2013): Summary of exploration geochemical and mineralogical studies at the Giant Pebble porphyry Cu-Au-Mo deposit, Alaska:

implications for exploration under cover; Economic Geology, v. 108, no. 3, p. 495–527, URL <https://doi.org/10.2113/econgeo.108.3.495>.

Fawcett, S.E. and Jamieson, H.E. (2011): The distinction between ore processing and post-depositional transformation on the speciation of arsenic and antimony in mine waste and sediment; Chemical Geology, v. 283, no. 3, p. 109–118, URL <https://doi.org/10.1016/j.chemgeo.2010.02.019>.

Flude, S., Haschke, M. and Storey, M. (2017): Application of benchtop micro-XRF to geological materials; Mineralogical Magazine, v. 81, no. 4, p. 923–948, URL <https://doi.org/10.1180/minmag.2016.080.150>.

Galloway, J.M., Swindles, G.T., Jamieson, H.E., Palmer, M., Parsons, M.B., Sanei, H., Macumber, A.L., Patterson, R.T. and Falck, H. (2018): Organic matter control on the distribution of arsenic in lake sediments impacted by ~~65 years of gold ore processing in subarctic Canada; Science of The Total Environment, v. 622–623, p. 1668–1679, URL <https://doi.org/10.1016/j.scitotenv.2017.10.048>.

Gent, M., Menendez, M., Toraño, J. and Torno, S. (2011): A review of indicator minerals and sample processing methods for geochemical exploration; Journal of Geochemical Exploration, v. 110, no. 2, p. 47–60, URL <https://doi.org/10.1016/j.gexplo.2011.05.005>.

Gonzalez-Alvarez, I., Goncalves, M.A. and Carranza, E.J.M. (2020): Introduction to the Special Issue Challenges for mineral exploration in the 21st century: targeting mineral deposits under cover; Ore Geology Reviews, v. 126, art. 103785, URL <https://doi.org/10.1016/j.oregeorev.2020.103785>.

Gottlieb, P., Wilkie, G., Sutherland, D., Ho-Tun, E., Suthers, S., Perera, K., Jenkins, B., Spencer, S., Butcher, A. and Rayner, J. (2000): Using quantitative electron microscopy for process mineralogy applications; Journal of the Minerals, Metals and Materials Society, v. 52, no. 4, p. 24–25, URL <https://doi.org/10.1007/s11837-000-0126-9>.

Hennekam, R., Sweere, T., Tjallingii, R., de Lange, G. J. and Reichart, G.-J. (2019): Trace metal analysis of sediment cores using a novel X-ray fluorescence core scanning method; Quaternary International, v. 514, p. 55–67, URL <https://doi.org/10.1016/j.quaint.2018.10.018>.

Hussain, M., Amao, A.O., Al-Ramadan, K., Babalola, L.O. and Humphrey, J.D. (2022): Unconventional reservoir characterization using geochemical signatures: examples from Paleozoic formations, Saudi Arabia; Marine and Petroleum Geology, v. 143, art. 105770, URL <https://doi.org/10.1016/j.marpetgeo.2022.105770>.

Hussain, M., Amao, A.J., Jin, G. and Al-Ramadan, K. (2018): Linking geochemical and mechanical properties of rock samples using new non-destructive techniques; Kingdom of Saudi Arabia Annual Technical Symposium and Exhibition, Society of Petroleum Engineers, April 23–26, 2018, Dammam, Saudi Arabia, Paper no. SPE-192347-SPE, URL <https://doi.org/10.2118/192347-MS>.

Jansen, J.H.F., Van der Gaast, S.J., Koster, B. and Vaars, A.J. (1998): CORTEX, a shipboard XRF-scanner for element analyses in split sediment cores; Marine Geology, v. 151, no. 1, p. 143–153, URL <https://doi.org/10.1016/S0025-3227(98)00074-7>.

Jooshaki, M., Nad, A. and Michaux, S. (2021): A systematic review on the application of machine learning in exploiting mineralogical data in mining and mineral industry; Minerals, v. 11, no. 8, p. 816, URL <https://doi.org/10.3390/min11080816>.

Jordan, M.I. and Mitchell, T.M. (2015): Machine learning: trends, perspectives, and prospects; Science, v. 349, no. 6245, p. 255–260, URL <https://doi.org/10.1126/science.aaa8415>.

Kanngieβer, B. (2003): Quantification procedures in micro X-ray fluorescence analysis; Spectrochimica Acta Part B: Atomic Spectroscopy, v. 58, no. 4, p. 609–614, URL <https://doi.org/10.1016/S0584-8547(02)00281-1>.

Kim, J.J., Ling, F.T., Plattenberger, D.A., Clarens, A.F. and Peters, C.A. (2022): Quantification of mineral reactivity using machine learning interpretation of micro-XRF data; Applied Geochemistry, v. 136, art. 105162, URL <https://doi.org/10.1016/j.apgeochem.2021.105162>.

Lougheed, H.D., McClenaghan, M.B., Layton-Matthews, D. and Leybourne, M. (2020): Exploration potential of fine-fraction heavy mineral concentrates from till using automated mineralogy: a case study from the Izok Lake Cu–Zn–Pb–Ag VMS deposit, Nunavut, Canada; Minerals, v. 10, no. 4, p. 1–33, URL <https://doi.org/10.3390/min10040310>.

McClenaghan, M.B. (2005): Indicator mineral methods in mineral exploration; Geochemistry: Exploration, Environment, Analysis, v. 5, no. 3, p. 233–245, URL <https://doi.org/10.1144/1467-7873/03-066>.

McClenaghan, M.B. and Layton-Matthews, D. (2017): Application of indicator mineral methods to bedrock and sediments; Exploration '17: Sixth Decennial International Conference on Mineral Exploration, October 22–25, 2017, Toronto, Ontario; Geological Survey of Canada, Open File 8345, 86 p., URL <https://doi.org/10.4095/306305>.

McClenaghan, M.B., Thorleifson, L.H. and Dilabio, R.N.W. (2000): Till geochemical and indicator mineral methods in mineral exploration; Ore Geology Reviews, v. 16, no. 3–4, p. 145–166, URL <https://doi.org/10.1016/S0169-1368(99)00028-1>.

Peti, L., Augustinus, P.C., Gadd, P.S. and Davies, S.J. (2019): Towards characterising rhyolitic tephra layers from New Zealand with rapid, non-destructive μ-XRF core scanning; Quaternary International, v. 514, p. 161–172, URL <https://doi.org/10.1016/j.quaint.2018.06.039>.

Plouffe, A., Ferbey, T., Hashmi, S. and Ward, B.C. (2016): Till geochemistry and mineralogy: vectoring towards Cu porphyry deposits in British Columbia, Canada; Geochemistry: Exploration, Environment, Analysis, v. 16, no. 3–4, p. 213–232, URL <https://doi.org/10.1144/GEOCHEM2015-398>.

Ryan, C.G., Kirkham, R., Moorhead, G.F., Parry, D., Jensen, M., Faulks, A., Hogan, S., Dunn, P.A., Dodanwela, R., Fisher, L.A., Pearce, M., Siddons, D.P., Kuczewski, A., Lundström, U., Trolliet, A. and Gao, N. (2018): Maia Mapper: high definition XRF imaging in the lab; Journal of Instrumentation, v. 13, no. 03, art. C03020, 8 p., URL <https://doi.org/10.1088/1748-0221/13/03/C03020>.

Schulz, B., Sandmann, D. and Gilbricht, S. (2020): SEM-based automated mineralogy and its application in geo- and material sciences; Minerals, v. 10, no. 11, art. 1004, URL <https://doi.org/10.3390/min10111004>.

Sillitoe, R.H. (2010): Porphyry copper systems; Economic Geology, v. 105, no. 1, p. 3–41, URL <https://doi.org/10.2113/gsecongeo.105.1.3>.

Sylvester, P. (2012): Use of the Mineral Liberation Analyzer (MLA) for mineralogical studies of sediments and sedimentary rocks; Mineralogical Association of Canada, Mineralogical Association of Canada Short Course Series, v. 42, p. 1–16.